Numerical models of subduction based on experimental data from analogue models

Jeniffer López Barandica

Universidad del Norte

Área de Ciencias Básicas, Departamento de Física y Geo-Ciencias

Barranquilla, Colombia

2022

Numerical models of subduction based on experimental data from analogue models

Jeniffer López Barandica

Tesis o trabajo de investigación presentada(o) como requisito parcial para optar al título de:

Profesional en Geología

Director:

Camilo Montes, PhD

Codirector:

Andrés Rodríguez-Corcho, Candidato a PhD

Línea de Investigación:

Modelamiento numérico y Geología estructural

Universidad del Norte

Área de Ciencias Básicas, Departamento de Física y Geo-Ciencias

Barranquilla, Colombia

2022

Like everything in my life, I dedicate this work to God. To my parents, who have always given me their support and unconditional love. And to myself, for having the determination, strength to overcome and for taking advantage of the opportunities that life has given me.

Acknowledgments

I thank the group of professors who taught me with care throughout my university career. Thanks to my thesis director, Camilo Montes, for his great interest, patience, teachings, and timely advice. To my thesis co-director, Andrés Rodriguez-Corcho, for involving me in the numerical methods and helping me at any time of the day.

Thanks to my family members, to my boyfriend, friends and colleagues who together formed a team to give me the necessary strength when I hesitated along the way, and they were always there with me.

Thank you all.

Abstract

In this work, three numerical models which capture plate-like behaviors were developed with a simple methodology that is based on experimental data from analogue models to promote the use in undergraduate students. To demonstrate the compatibility of analogue modeling and numerical modeling software that runs in personal computers, three models were ran changing the boundary conditions of the bottom, and the lithosphere layer shape to evaluate its influence. Model 1 and Model 2 had two different events of subduction, taking 15 hours to initiate the motion and 11 minutes in the geodynamic events; while Model 3 had four different events, taking 40 minutes to initiate motion and 15 minutes of action. Model 1 was the base model with a free-slip boundary condition at the bottom that promoted higher speeds (maximum ~ 1.2e7 cm/s), smoother lithosphere subduction, and further advancement of the trench during the first slab subduction. Model 2 had a non-slip boundary condition which caused slab folding as soon as the slab hit the bottom and this promoted earlier thinning and tearing, less duration of trench advance and lower trench speeds (maximum ~ 1e7). Finally, Model 3 with a gap of 2 cm at the right edge of the lithosphere layer allowed the system to have lower values of velocity than the other two models (maximum ~ 7e6), less time to initiate the motion in the dynamic system, and more uniformity in results, such as viscous dissipation with correlated peaks in terms of the different events of subduction. All models had similar behaviors of the base analogue model, in terms of multiple slab tearings. However, Model 3 is the one that has a better resemblance to the analogue model in terms of time scale.

Keywords: Numerical modeling, analogue modeling, subduction, slabs, undergraduate students.

Resumen

En este trabajo, desarrollé tres modelos numéricos que capturan comportamientos de placas tectónicas con una metodología simple que se basa en datos experimentales de modelos análogos, para promover el uso en estudiantes de pregrado. Para demostrar la compatibilidad del modelamiento análogo y el software de modelamientos numéricos ejecutado en computadores personales, ejecuté tres modelos cambiando las condiciones de frontera del fondo y la forma de la capa de la litosfera para evaluar su influencia. El Modelo 1 y el Modelo 2 tuvieron dos eventos diferentes de subducción, tardando 15 horas en iniciar el movimiento y 11 minutos en los eventos geodinámicos; mientras que el Modelo 3 tuvo cuatro eventos diferentes, tardando 40 minutos en iniciar el movimiento y 15 minutos de acción. El modelo 1 fue el modelo base, con una condición de frontera de deslizamiento libre en la parte inferior que promovió velocidades más altas (máximos ~ 1.2e7 cm/s), una subducción de litosfera más suave y un mayor avance de la trinchera durante la subducción del primer slab. El Modelo 2 tenía una condición de frontera con fricción, que causaba el plegado del slab tan pronto como éste tocaba el fondo, por lo cual promovía un adelgazamiento y desgarro más temprano, una menor duración del avance de la trinchera y velocidades de trinchera más bajas (máximos ~ 1e7). Finalmente, el Modelo 3 con una brecha de 2 cm en el borde derecho de la capa de la litosfera permitió que el sistema tuviera valores de velocidad más bajos que los otros dos modelos (máximos ~ 7e6), menos tiempo para iniciar el movimiento en el sistema dinámico y más uniformidad en los resultados, como la disipación viscosa con picos correlacionados en términos de los diferentes eventos de subducción. Todos los modelos tuvieron comportamientos similares al modelo análogo base, en términos de desgarros múltiples del slab. Sin embargo, el Modelo 3 es el que tiene un mayor parecido con el modelo análogo en términos de escala de tiempo.

Palabras Clave: Modelamiento numérico, modelamiento análogo, subducción, slabs, estudiantes de pregrado.

Content

List of figures

List of tables

List of symbols

Symbol	Term	Definition
Φ	Viscous dissipation	Equation 4.1
$\dot{y}$	Shear strain rate	Equation 4.1
τ	Shear stress	Equation 4.1

Introduction

Numerical models are a powerful tool to investigate tectonic and geodynamic processes that occur at geological timescales. Over time, the representation of geological processes has contributed to the resolution of problems that could be too complex to be resolved because of the large spatial-time scales (Capitanio et al., 2021). Previous research has developed computationally complex numerical simulations of mantle convection in 2-D (Moresi et al., 2002; Moresi et al., 2003; Cooper et al., 2004; Capitanio et al., 2007; Yang et al., 2019; Faccenna et al., 2021), and 3-D (Moresi et al., 2007; Schellart et al., 2013; Moresi et al., 2014; Zhang et al., 2017). One of the topics investigated with numerical models is the process of subduction, where researchers have already solved many of the techniques and parameters (Gerya, 2022). However, numerical models are computationally expensive, limiting their use in undergraduate studies.

In this project, the use of computationally simple and inexpensive numerical models is demonstrated using data from an undergraduate class-project analogue model. A personal computer was used to perform numerical models that explore diverse parameters such as plate thickness, the effect of viscosity contrasts, density contrasts, strength, and the role of boundary conditions. I compared the numerical data with data obtained in simple analogue models, such as trench-advance velocity and subducted area at a specified time. The purpose of this work is to get undergraduate students closer to the development of numerical models, providing a template that can be used by students in undergraduate Structural Geology classes to better understand Earth geodynamics. With these simple numerical models, students will have the possibility to run their own models, observing the impact of changes in parameters in the dynamic evolution.

My numerical models capture plate-like behaviors with a simple methodology that is based on experimental data from analogue models. The results are numerical representations of subduction processes. In the results section, the temporal evolution of the subducted slab, the subducted area,

the surface kinematics, the plastic strain field, and viscous dissipation are evaluated. Finally, the outcomes are discussed taking into consideration the differences between analogue model and numerical models results, and evaluate the influence of parameters used, relating concepts and theory to observations.

1. Theoretical framework

Results of previous models, both analogue and numerical, have considered distinct parameters to study different subduction processes. Funiciello et al. (2003, 2004), Martinod et al. (2005), and Regard et al. (2005), performed analogue models with honey to study subduction of an oceanic lithosphere with buoyant ridges or plateaus, the impact of deep subducting plates on indentation, or the classification of dynamic results based on presence of open or closed boundary conditions. Stegman et al. (2010) used 3-D numerical models to propose differences in subduction dynamics by varying the strength of slabs as well as the buoyancy. Capitanio et al. (2010), instead used 2-D models that consider the influence of overriding plate feedbacks into the dynamics of subduction.

Since the first authors decided to develop 2-D numerical geodynamic models, subduction has been the most studied and analyzed geodynamic process with computational tools (Gerya, 2011). Development of computational equipment provided an important tool to the solution of scientific problems. Numerical methods are given by equations that govern geodynamic processes. Considering the mantle behavior as a viscous fluid for the geological time scales, governing equations based on the conservation laws describe the flow of highly viscous fluid (Ismail-Zadeh et al., 2010). Basically, conservation of mass, conservation of momentum, conservation of energy and rheological law are equations that govern mantle and lithosphere dynamics.

Underworld2 is a Lagrangian-particle in-cell finite code that solves the Stokes and momentum equations and consists of a Python-based, high performance, parallel code that can be used in personal computers and high-performance computers (Beucher et al., 2019). This numerical method considers the tracking of materials as they are subjected to deformation due to the involved flow and provides important information about the dynamic behavior.

Sobolev et al. (2005) states that a visco-elasto-plastic rheology enables the production of more realistic topographic profiles throughout subduction simulations with numerical methods. Even though the superficial layer in the analogue model I want to reproduce was a Mohr-Coulomb material, it probably turned into a viscous fluid because of absorption of the viscous fluid below. In this work, the materials used in the analogue model are represented as visco-elasto-plastic fluids because a Mohr-Coulomb material cannot be accounted in the Stoke's equation used by *Underworld2* to compute the numerical simulations.

2. Problem statement

Numerical modeling of geological processes has been used for approximately 50 years in engineering sectors as well as in academic research. The advance of technology and improvement on computational high-performance infrastructure have contributed to the development of sophisticated numerical models, receiving much wider acceptance both in research and in routine engineering practice (Stead et al., 2006). Application of numerical models is essential for geoscientists to understand processes that occur at geological timescales. However, it is almost impossible for a geoscience student to create a numerical model that could capture the first-order Earth dynamics. Numerical models represent Earth dynamics as a simulation of basic geophysical processes and phenomena (Ismail-Zadeh et al., 2010).

Even though numerical models are simplified compared to geodynamic observations, the models are still complex and expensive to build and run. To develop geodynamics numerical models, it is usually necessary to have time in a high-performance computational facility, not usually available for undergraduate students. Consequently, all of this represents a big limitation for undergraduate students, because of the difficult access to high-performance computational infrastructure.

It is important to promote in undergraduate students the interest for numerical models and bring them closer to that experience, providing students the tools they need to start. Considering the advance in technology and science, numerical models are important for acquiring new knowledge and understanding of geodynamics processes. If we introduce these concepts early, as an easy and cheap alternative, many students would be involved in it, exploring new possibilities, and gradually immersing themselves into global geodynamic problems.

3. Objectives

3.1. General objective

To demonstrate and promote in undergraduate students the development of simple and accessible numerical models, to bring them closer to these tools that contribute to the understanding of geodynamic processes.

3.2. Specific objectives

- To develop simple numerical models with minor differences in some variables to evaluate their influence, using data obtained from subduction analogue models.
- To contrast the results obtained in models with experimental data to verify whether they properly represent geodynamic processes.
- To provide a simple numerical model template for students to learn about geodynamics, interact and modify parameters from their personal computers.

4. Methodology

In order to promote numerical modeling for the undergraduate community, I developed subduction geodynamic models based on previous analogue modeling performed during a Structural Geology class. I highlight the ease that this methodology would represent for undergraduate students, allowing them to visualize and quantify in a dynamic way, how the Earth lithosphere and mantle is deformed by the process of subduction. Furthermore, the numerical modeling work presented in this thesis will enable undergraduate students to start developing numerical models in the future.

4.1. Analogue model assembly

An analogue model of subduction developed for a structural geology class project (Delgado et al., *in review)* was used as a starting point for the numerical simulations. The analogue model consisted of the use of white school glue and black magnetic sand to simulate the sub-lithospheric mantle and a subducting plate, respectively. This model also included another type of sand with a contrasting color to track deformation. The analogue model was recorded and ran for 6 min 36 s before starting the subduction process which had additionally a duration of 1 min 26 s. From the recorded video, images of the dynamic part were extracted each 2 s obtaining 44 images (see **Figure A-1**). The pictures were exported to ImageJ (rsb.info.nih.gov/ij) to generate graphics with subducted area information (see **Figure A-2**). In addition, general data about the assembly is shown in **Table 4-1**, such as viscosity, density, thickness, weight, and grain size.

Table 4-1: Materials used and their physical properties. All measurements made with kitchen.

Material	Weight (g)	Density (kg/m^3)	Grain-size (mm)	Viscosity (Pa.s)	Thickness (cm)
School glue	605	1027	--	21.7	6
Magnetic sand	260	2286	0.3-0.4	--	0.8
Quartz sand	30	1550	0.9-1.2	--	--

4.2. Numerical model

My numerical models are based on the above-mentioned analogue model, in which mechanical properties, such as viscosity and density were experimentally measured, which means the computational models represented in this project are based on real parameters and observations. However, it was necessary to include additional information on scripts to develop the models, such as magnetic sand layer viscosity, plasticity, time scales and generation of passive tracers.

4.2.1. Parameters

To initiate the numerical model's assembly, it was essential to define the parameters to use. I tested different values for viscosity, density, plasticity, and plate thicknesses. After some testing runs, I set the parameters to be used considering established concepts and theory (see **Table 4-2**).

First, magnetic sand as lithosphere, and school glue as upper mantle, are both considered viscous materials because of software limitations, in particular the magnetic sand layer needed to be considered as visco-elastic material to observe the viscous and elasticity properties after being subjected to deformation. For that reason, it was necessary to derive an appropriate viscosity value for the upper layer. Numerical models tests with lithospheric proportions (two orders of magnitude difference between continental lithosphere and upper mantle; Walcott, 1970) did not work properly, so I decided to test with double of it and better results were achieved. It was also

necessary to define the plasticity properties, taking into consideration the real material properties on Earth, after some testing sessions to find the value that better worked with my numerical model dimensions and properties, the optimal results were obtained with a cohesion of 50 Pa and a cohesion after softening of 30 Pa.

On the other hand, layer thicknesses were a close representation of the real proportion on Earth, because in the analogue model the lithosphere is made up of 0.8 cm while sub-lithospheric mantle had 6 cm, so they almost maintained the proportion of 100 km for lithosphere and 660 km discontinuity (Shearer, 1990). Then layers dimensions of numerical models were established after testing sessions, finding out the best thickness for the upper layer was 1 cm (see **Figure 4- 1**).

Table 4-2: Initial parameters used to develop the numerical models.

Parameter	**Value**
Upper layer density (kg/m^3)	2286
Lower layer density (kg/m^3)	1027
Upper layer viscosity (Pa.s)	10000 (21.7)
Lower layer viscosity (Pa.s)	21.7
Upper layer Thickness (cm)	1
Box dimensions (cm)	28 x 6.8
Resolution	0.2 x 0.075 cm per element
Slab plasticity (Pa)	Cohesion = 50
	Cohesion after softening = 30

Figure 4-1: Layer thicknesses. In red: lithosphere. In blue: asthenosphere.

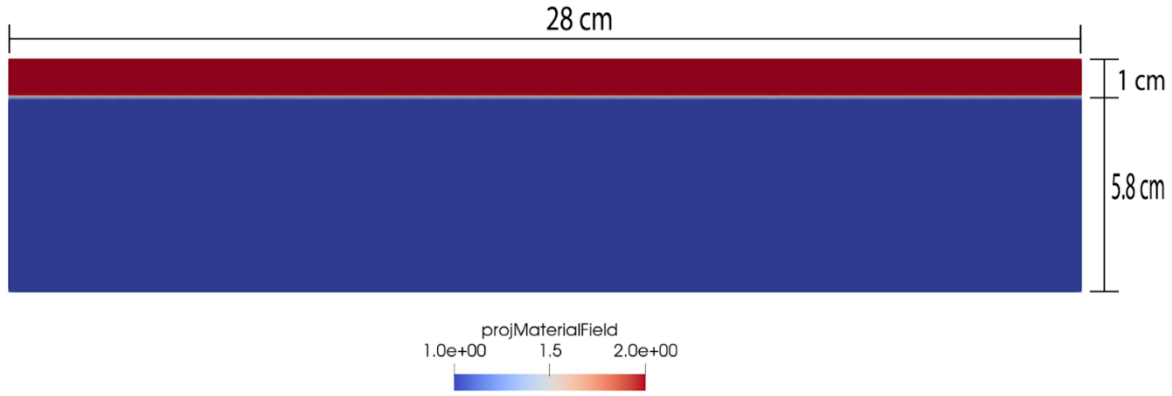

4.2.2. Passive tracers

Passive tracers are individual points that store information over time about location and velocities in models. To have a better understanding and visualization of geodynamic processes I included three rows of passive tracers in the upper layer (see **Figure 4- 2**) to have the possibility to evaluate most of the trench behavior.

Figure 4-2: Image of the location and organization of passive tracers (black dots). In red: lithosphere. In blue: asthenosphere.

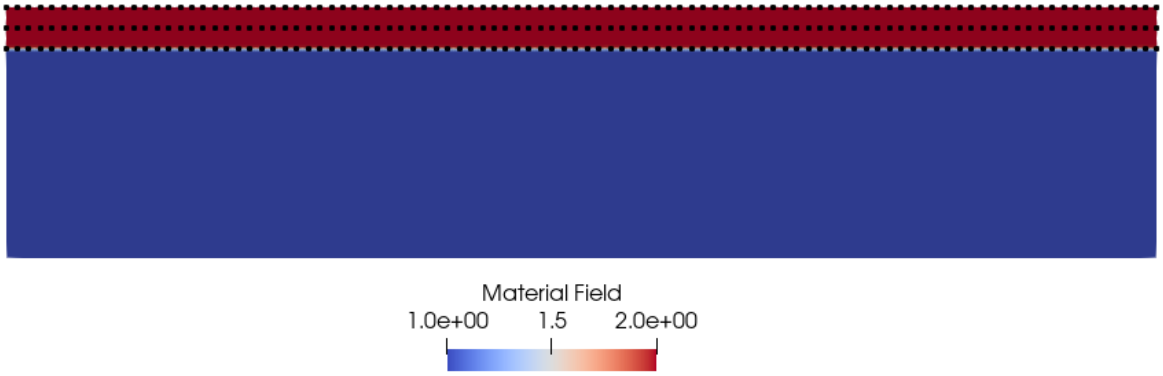

However, I used the tracer that best represented the flow and allowed me to understand the dynamic of the models (see **Figure 4-3**). With the information that I extracted from the chosen tracer I made graphs of Trench-Advance that provide the velocities that each model had along the time.

Figure 4-3: Image of the location selected of the passive tracer used to measure the trench-advance velocity (black dot). In red: lithosphere. In blue: asthenosphere.

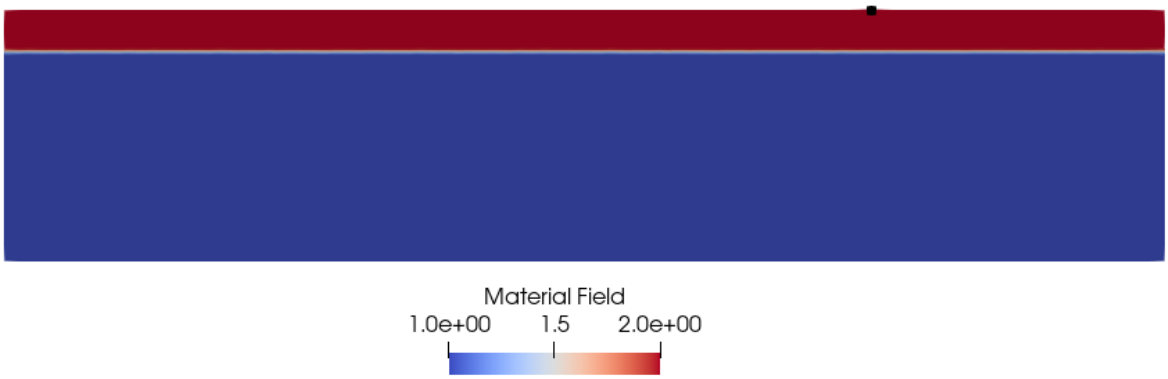

4.2.3. Software and processes

To develop the numerical models, I used my personal student computer model HP Laptop 14-bs0xx, OS Microsoft Windows 10 Home Single Language, Intel(R) Core (TM) i3-6006U CPU @ 2.00GHz, 1992 Mhz, 2 main processors, 4 logical processors, (RAM) 8,00 GB.

I developed numerical models in the Underworld/UWGeodynamics code in its version 2.10.2 (underworldcode.org) using the web-based interactive computing platform Jupyter Notebook (jupyter.org) and Python 3.9. After having data in folders, it was visualized and analyzed by time steps in the open-source Paraview (paraview.org).

Paraview enables the visualization of the material field, stress tensor, plastic strain field and the velocity vectors. To show velocity vectors it was necessary to click on the Glyph option and use the properties window to modify size, color, or any characteristic of vectors.

Values of viscous dissipation represent the energy that is produced due to the action of shear forces that deform a viscous fluid. In this work, I used the second invariants of the stress and strain tensors in the calculator tool to report the viscosity dissipation, following the equation (see **Equation (4.1)**) suggested by Holtzman et al. (2005). Although the values of this property are represented in W/m^2, it was necessary to use the 'Integrate Variables' tool to integrate the values

obtained in the whole model to generate a single value per step, so the unit obtained and shown is W/m.

$$\Phi = \tau * \dot{y} \qquad \textbf{(4.1)}$$

After that, using the option Filters > Data analysis > Integrate variables, I queried the subducted area. Information contained on passive tracers yielded the trench velocity over time by clicking on Information > Data arrays. Also, it was possible to extract all that information in .csv files, which needed to be slightly modified in a spreadsheet to make graphics of variables vs time in Jupyter Notebook. Graphs shown are about velocity trench, plastic strain in upper layer (subducting plate) and strain rate for each layer and complete model.

4.2.4. Models

I developed three models with the same basic data in assembly (see **Table 4-2**), but minor differences to evaluate the influence of boundary conditions and lithosphere layer shape. All models are composed of two layers: the top layer in all models is composed of a material with density of 2286 kg/m^3, viscosity of 217e3 Pa.s, thickness of 1 cm, and plasticity properties with cohesion of 50 Pa and cohesion after softening of 30 Pa. The bottom layer is composed of a material with density of 1027 kg/m^3, viscosity of 21.7 Pa.s and thickness of 5.8 cm. The resolution used for all models was 0.2 x 0.075 cm per element.

The boundary condition on the right-hand side of the box has a frictionless behavior, while the left-hand side has a friction behavior. In the bottom, I set a frictionless behavior as default, however I changed that parameter in one of the models to evaluate its influence.

Every model was in action at their own time scales. Something in common is that they took a long time to start in comparison with the total time of action. So, the first part of all models saved checkpoints at larger time scales and in subduction events the checkpoints were saved at smaller time intervals.

In all models the plots about subducted area, subduction rate and viscous dissipation of the lithosphere are made with data of a cross-section, where I considered the values of subduction were taken below the 2 cm of depth in the model. This, to avoid getting information about parts of the lithosphere that could never subduct.

5. Results and Analysis

5.1. Results

The objectives and results of this work represent a new outlook of numerical models, giving examples and tools to undergraduate students, which they could use to develop their own numerical models and explore them with different parameters. For that reason, I provide a practical guide to Geology Students (see **Appendix B**) with instructions of software downloads, access, and Python scripts to run basic models with their preferences. The first model is the point of reference for the next models, so I ran one model with the basic properties I described above, and the second and third models were run with minor differences.

5.1.1. Model 1

This model (see Model 1.mpg) was initially run for a duration of 15 hours with a checkpoint every 1 hour. I then restarted the model to run for another 11 minutes with a checkpoint every 5 seconds, this process was necessary to better observe the dynamics of the model. In this model, two different events of subduction were formed. The lithosphere took around 13 hours to start weakening (see **Figure 5-1a**) and for around the 15 hours the zones of weakness showed smaller values of viscosity and stress tensor (see **Figure 5-1b**). However, it was not until 15 hours and 7 minutes approximately that the first event of subduction was initiated. That first event had a duration of 45 seconds until the slab began to thin out (see **Figure 5-1c and 5-1d**). After that, the poloidal flow in the system promoted the drop of another slab (see **Figure 5-1e**), which had a duration of 55 seconds until it had a breakthrough and ended the action having a slight trench retreat during the last 20 seconds of motion. The highest values of plastic strain were given in the zones where the slab had extension as it was being subducted. This model was frictionless at the bottom, so this property allowed the slabs to slip easily once they reached the bottom of the experiment. The model ends up with unsubducted lithosphere parts on each side (see **Figure 5-1f**).

Figure 5-1: Selected image captures of the evolution of Model 1. The upper panel in each figure represents the viscosity field in the model, the middle panel represents the horizontal normal stress tensor field, the bottom panel shows the two materials in the model and in shades of orange the plastic strain field is represented. Black arrows represent poloidal flows within the asthenosphere induced by the sinking slab.

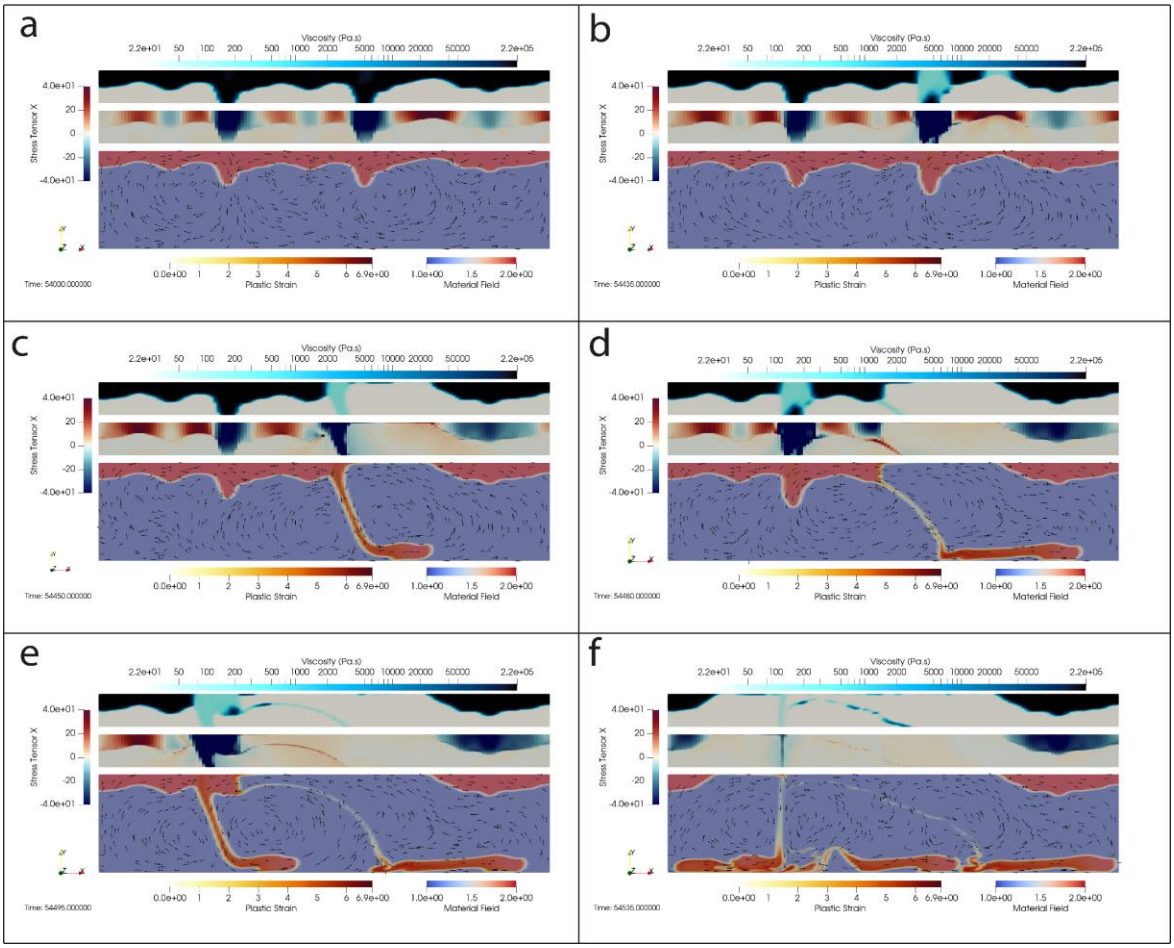

The trench advance of this model showed velocities with speeds of 1e7 cm/s, that reaches values of 1.2e7 cm/s in the first peak that occur after 15.12 hours (see **Figure 5-2a**), which corresponds to the first event of subduction observed in the model. Then, at 15.13 hours the trench velocity slows down, and after that increases again reaching 1.2e7 cm/s, but then decreases to less than 1e7 and immediately reaches its high value again, and finally stops abruptly at 15.14 hours. Subsequently, the direction of the movement slightly changed at the end of the model; this episode is related to a trench retreat that reaches around 0.2e7 cm/s. In general, the first event of subduction was a single

event with a linear behavior, but the second event of subduction contained 3 fluctuations that could be described as 3 sub-events.

Plastic strain plot (see **Figure 5-2b**) has an almost linear behavior that initiates in minimum value of 0 and ends at a maximum value of 5.5e-9 approximately. The plot presents a small curvature that separates the two different subduction events, given after 15.13 hours with a value of 2e-9, when the second event initiates. When the second event ends, after 15.15 hours, the values of plastic strain become almost constant and kept like that until the model is finished. So, the maximum value of plastic strain reached, represents the plastic deformation found in this dynamic system. The plastic strain is given as the slabs are being affected by the flows causing its elongation during dynamic and compression after being close to the bottom.

Viscous dissipation plots are made from total model and lithosphere information, to evaluate if they are similar or not (see **Figure 5-2c and 5-2d**). The behavior observed is that the peak viscous dissipation in the lithosphere (with values between ~ 2.5e-9 W/m and ~ 3.5e-9 W/m) are always lower than any peak value for the whole-model (maximums near 1.2e-8 W/m). In the viscous dissipation plot for the whole-model, the first event of subduction represents the higher values in the system, while the second event started with a high value but then progressively decreased to reach ~ 0.8e-8 W/m. On the other hand, in the viscous dissipation plot of the lithosphere, the first event represents the lower value with ~ 2.5e-9W/m, while the second event represents a progressive increase in values that reach ~ 3.5e-9 W/m.

The subducted area plot (see **Figure 5-2e**) shows the cumulative area of the lithosphere that is subducted with time. The lithosphere started to be subducted after the 15.12 hours and the area subducted reached the 10 cm^2 in the first event that ended after the 15.13 hour, giving way to the second event. That second event consumed around 15 cm^2 of lithosphere area, so when the motion was finished, at 15.15 hours approximately, the subducted area kept constant with a total of 25 cm^2. The behavior of the subducted area plot is related to the plastic strain plot because the more lithosphere area is subducted the more material is deformed.

Finally, the subduction rate plot (see **Figure 5-2f**) shows that the first event of subduction contained the largest subducted area in a single event, because the rest of the area was subducted during the second event of subduction which included 3 sub-events. So, the first peak that surpasses the 0.4 cm^2 is related to the first event. And then, the second event contains two sub-events after 15.13 until 15.14 hours that also reach 0.4 cm^2, but the third sub-event was below 0.3 cm^2. At the end, after 15.15 hours it is not more area subducted.

Figure 5-2: Information plots about the time evolution of Model 1: a) Trench Advance, b) Plastic Strain, c) Viscous Dissipation of total model Asthenosphere-Lithosphere, d) Viscous Dissipation of Lithosphere only, e) Subducted area and f) Subduction Rate.

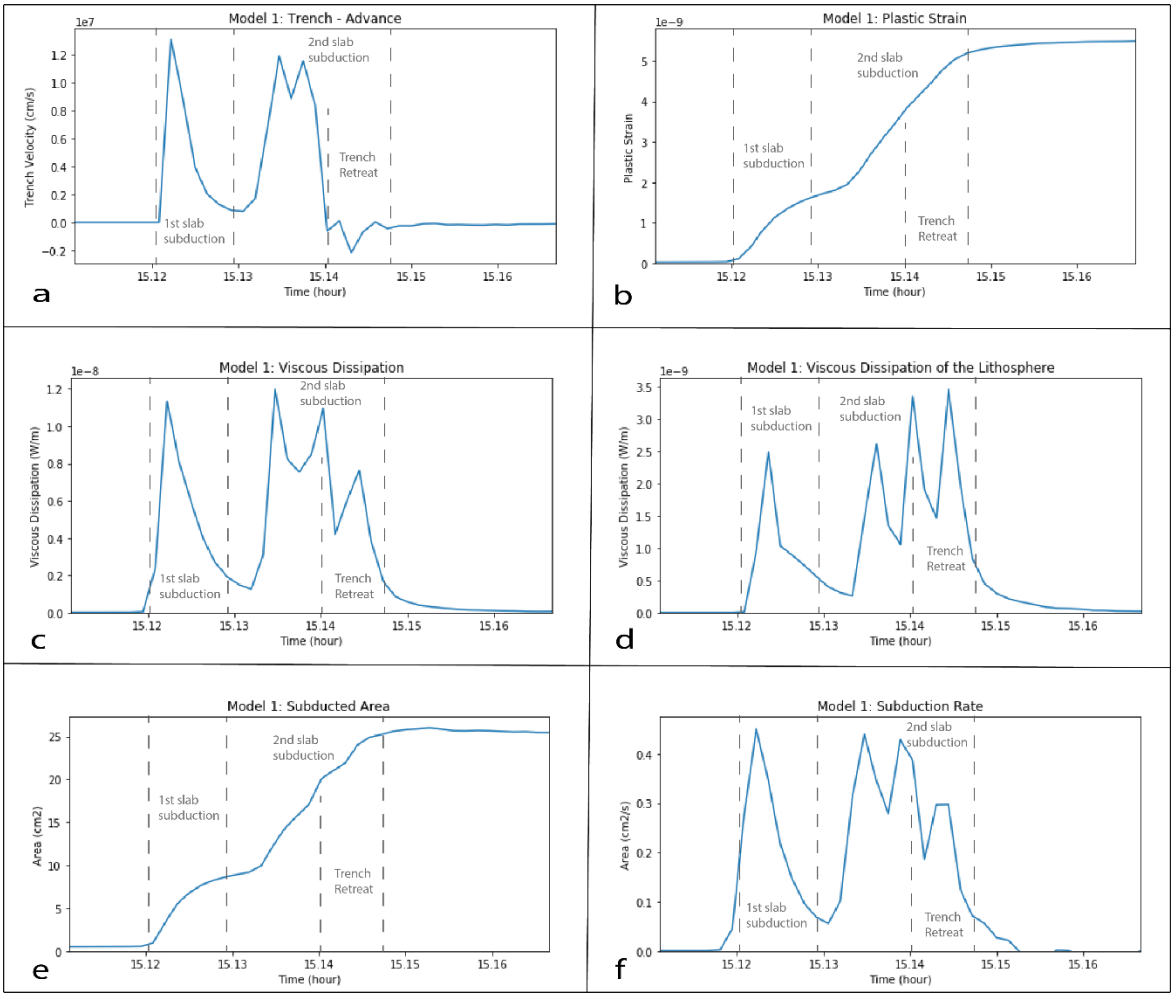

5.1.2. Model 2

The second model (see Model 2.mpg) was initially run for a duration of 15 hours with a checkpoint every 1 hour. Then, I restarted the model to run another 11 minutes with a checkpoint every 5 seconds, so in total the model ran for 15 hour 11 minutes. I changed the parameter of the bottom boundary condition in this model, so the bottom is frictional to evaluate the behavior of slabs with this property.

The model presents two different events of subduction. In this case, the lithosphere also took around 13 hours to start the weakening (see **Figure 5-3a**) and took for around 15 hours to present clearly zones of weakness reflected in viscosity and stress tensor values (see **Figure 5-3b**). The motion initiated at 15 hours 7 minutes approximately with the first event of subduction (see **Figure 5-3c**). This first event had a duration of 40 seconds until the slab began to thin out (see **Figure 5-3d**). While the first slab was breaking up, the flows in the system helped to initiate another event of subduction (see **Figure 5-3e**), which had a duration of 70 seconds until it had a breakthrough and ended the action. Approximately during the last 35 seconds of the second event of subduction, the model presented a trench retreat.

The maximum values for plastic strain were in slabs when going through elongation or compression. The frictional condition of the bottom did not allow the easy slip of slabs. The slabs tended to compress as soon as the bottom was reached. Like Model 1, this second model ends up with unsubducted lithosphere parts on each side of the box (see **Figure 5-3f**).

Figure 5-3: Selected image captures of the evolution of Model 2. The upper panel in each figure represents the viscosity field in the model, the middle panel represents the horizontal normal stress tensor field, the bottom panel shows the two materials in the model and in shades of orange the plastic strain field is represented. Black arrows represent poloidal flows within the asthenosphere induced by the sinking slab.

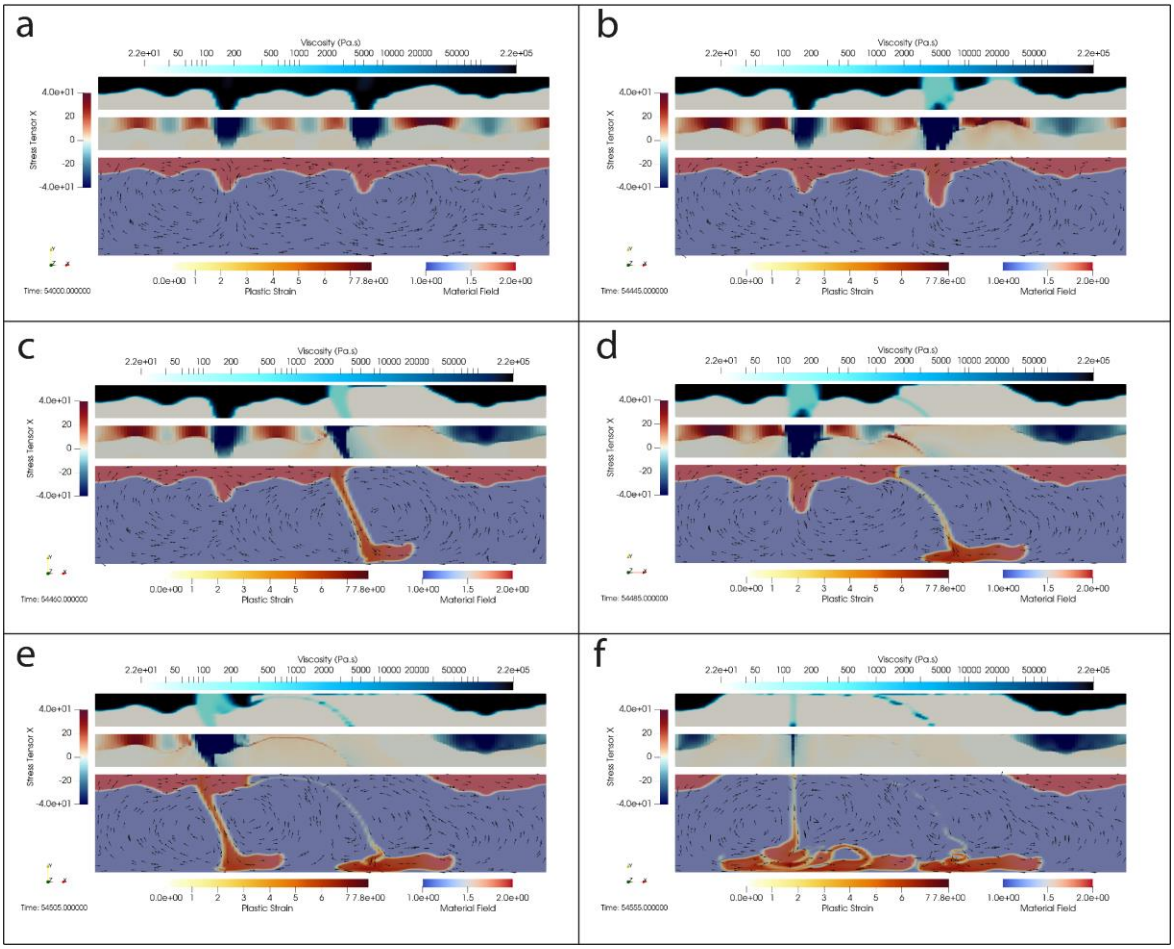

The trench advance of this model shows velocities with maximum speeds of 1e7 cm/s, that are reflected in the first peak that occur between 15.12 and 15.13 hours (see **Figure 5-4a**). This first peak represents the first event of subduction, so that is the fastest dynamic in the model. Then, at 15.13 hours the trench velocity slows down, and after that increases again before 15.14 hours almost reaching 1e7 cm/s, but then decreases to less than 0.6e7 and immediately reaches its high value again, and finally stops abruptly between 15.14 and 15.15 hours. Subsequently, the direction of the movement slightly changed at the end of the model, being related to a trench retreat that reaches less than 0.2e7 cm/s and shows fluctuation behavior until almost 15.16 hours.

The plastic strain plot (see **Figure 5-4b**) also has a linear behavior that initiates in 0 and ends at a maximum value of ~ 7e-9. In this case the plot does not show a significant curvature, however it is possible to observe a light intersection between 15.13 and 15.14 hours that is related with the end of the first event of subduction, having a value of ~ 2e-9. Since that moment, the values continue to increase until they reach the maximum value that is the total plastic deformation the system had.

Viscous dissipation plots (see **Figure 5-4c and 5-4d**) also demonstrate that the peak viscous dissipation in the lithosphere (with values between ~ 2e-9 W/m and ~ 3.5e-9 W/m) are always lower than any peak value for the whole-model (maximums near 1.2e-8 W/m). In the viscous dissipation plot of the lithosphere, the first event represents the lower value with ~ 2e-9W/m, while the second event represents a progressive increase that reaches ~ 3.5e-9 W/m between 15.13 and 13.15 hours. On the other hand, in the viscous dissipation plot for the whole-model, the first event of subduction represents the higher values in the system with ~ 1.2e-8 W/m, while the second event started with a high value but then progressively declined to reach less than ~ 0.6e-8 W/m.

The subducted area plot (see **Figure 5-4e**) shows that the lithosphere started to be subducted after 15.12 hours and the area subducted reached less than 10 cm^2 in the first event that ended between 15.13 and 15.14 hours. The second event, that also includes 3 sub-events, shows light intersections that allow the identification of the 3 peaks that are clearly observed in other plots. In total, the second event consumed around 15 cm2 of lithosphere area, so when the motion was finished, after 15.15 hours, the subducted area kept constant with a total of 25 cm2.

Eventually, the subduction rate plot (see **Figure 5-4f**) also shows that the first event of subduction contained the largest subducted area in a single event, because the rest of the area was subducted during the second event of subduction which included 3 sub-events. So, the first peak that almost reaches 0.4 cm2 is related to the first event. And then, the second event contains two sub-events after 15.13 until 15.15 hours that reach 0.4 cm^2 and 0.35 cm^2, respectively. But the third sub-event reached ~0.25 cm^2. At the end, at 15.16 hours it is not more area subducted.

Figure 5-4: Information plots about the time evolution of Model 2: a) Trench Advance, b) Plastic Strain, c) Viscous Dissipation of total model Asthenosphere-Lithosphere, d) Viscous Dissipation of Lithosphere only, e) Subducted area and f) Subduction Rate.

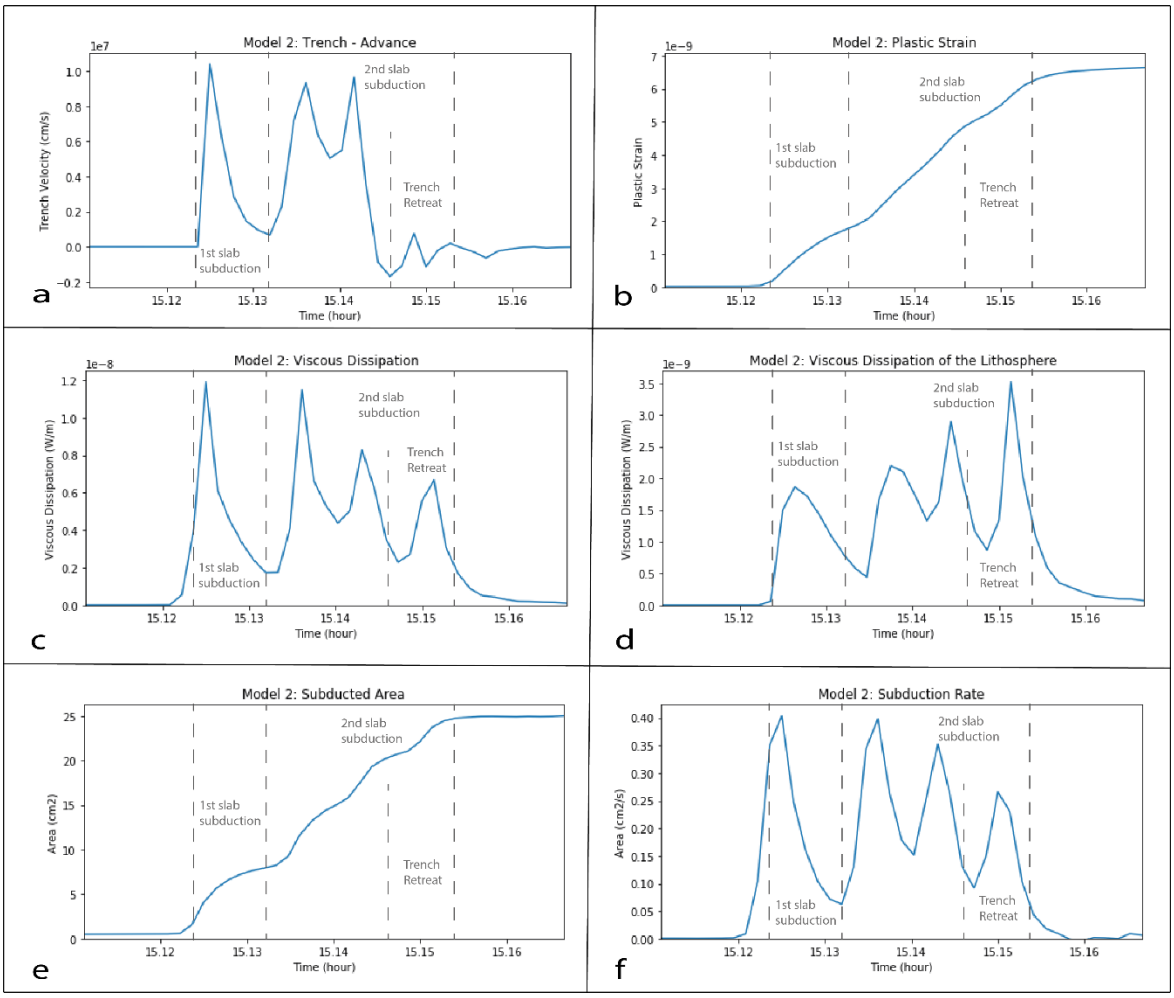

5.1.3. Model 3

The third model (see Model 3.mpg) was initially run for 40 minutes, saving checkpoints every 10 minutes. The action during this time was not so dynamic, so, I restarted the model to run another 20 minutes with a checkpoint every 15 seconds. In total the model ran for a duration of 60 minutes. Having the Model 1 as the base model, the Model 3 had a change in its lithosphere layer. In this case, the lithosphere layer has a gap of 2 cm on the right-hand side of the box to evaluate the behavior of flows and weak zones (see **Figure 5-5a**).

In general, this model presented 4 different events of subduction. Since the initial moment, the lithosphere started to have an advance without being subducted and took around 41.7 minutes to start the motion that evidenced the weak zones with low values of viscosity (see **Figure 5-5b**). In that moment, the first slab was formed and had a duration of 90 seconds until the slab began to thin out (see **Figure 5-5c and 5-5d**). After that, the lithosphere remained a trench advance without subduction for 240 seconds, until the initiation of the second event of subduction. The second slab subduction (see **Figure 5-5e**) had a duration of 60 seconds until it thinned out and broke. Then, another time interval of trench advance without subduction was presented for 360 seconds. Subsequently, the third slab subduction was promoted (see **Figure 5-5f**) and it also took 60 second until its breaking. Finally, the remaining part of the lithosphere was almost static (see **Figure 5-5g**) for 60 seconds before giving way to the last event of subduction (see **Figure 5-5h**) that had a duration of approximately 75 seconds. After that, the dynamic in the model was finished with a total duration of ~ 15.7 minutes.

Figure 5-5: Selected image captures of the evolution of Model 3. The upper panel in each figure represents the viscosity field in the model, the middle panel represents the horizontal normal stress tensor field, the bottom panel shows the two materials in the model and in shades of orange the plastic strain field is represented. Black arrows represent poloidal flows within the asthenosphere induced by the sinking slab.

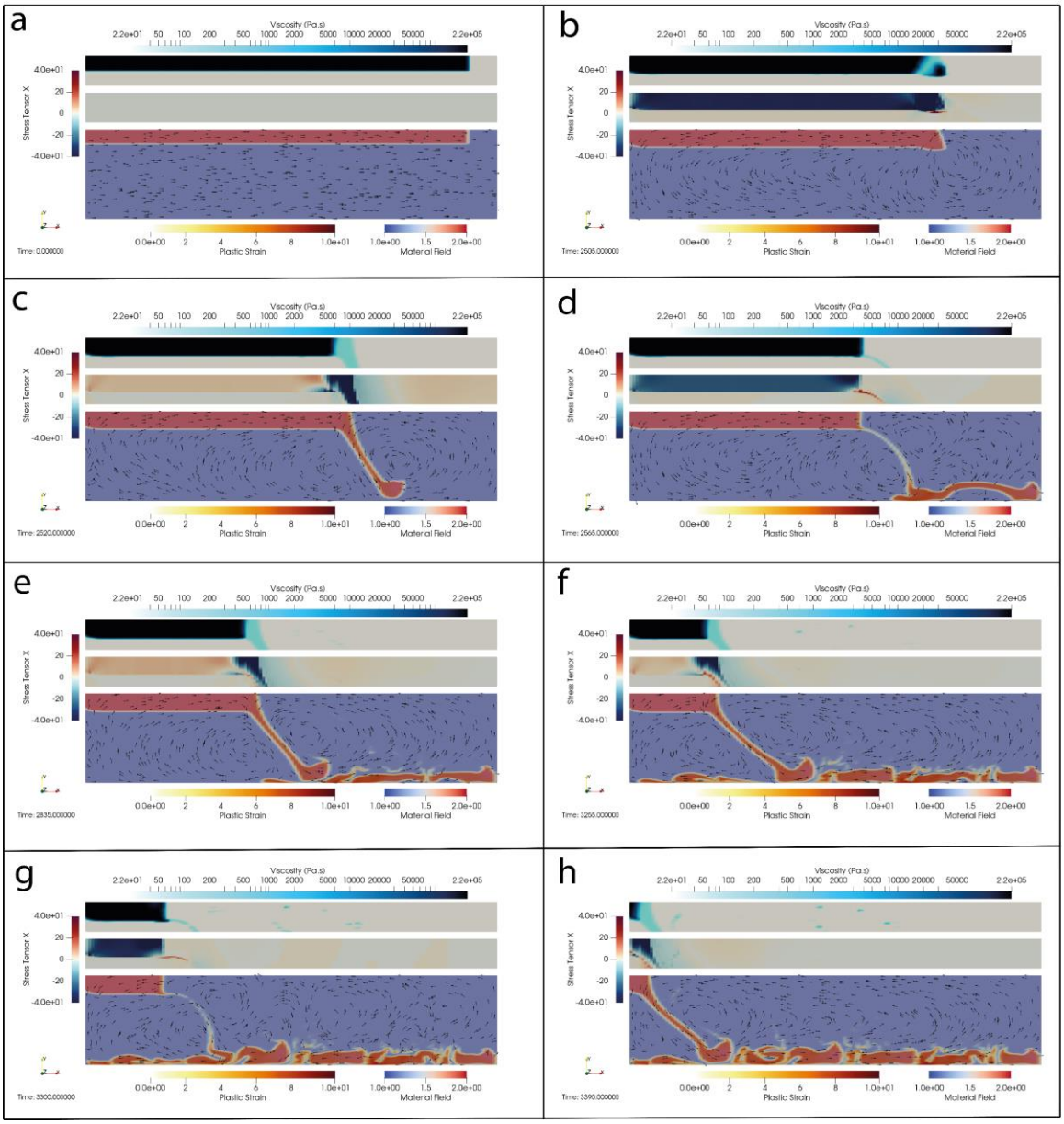

The trench advance plot (see **Figure 5-6a**) shows that this model reaches velocities with speeds of 1e6 cm/s. Considering that the third model has 4 different events of subduction and that they are

separated by time intervals without action, I will describe the 4 important peaks, without mentioning the time lapses that are not dynamics. So, the first event that occurred before 42.5 minutes reached 6e6 cm/s, the second peak surpassed 5e6 cm/s before 47.5 minutes, the third peak surpassed 7e6 cm/s between 52.5 and 55 minutes and the last one reached ~ 7e6 cm/s. The lower peak is the one that corresponds to the second event, while the higher peak corresponds to the third event of subduction.

The plastic strain plot (see **Figure 5-6b**) has a behavior that simulates stairs because of the events of subduction that are separated for inactive time lapses. The first increase is presented at 42.5 minutes reaching a value of 2e-9. Then, at 47.5 minutes the plastic strain value increased to ~ 4e-9 and remained constant until the third event at approximately 55 minutes, where it reached ~ 6e-9. Finally, around 57.5 minutes the plastic strain value surpassed the 8e-9 and remained until the dynamic was finished.

For this Model, viscous dissipation plots (see **Figure 5-6c and 5-6d**) have a different behavior in comparison with Model 1 and Model 2. In this case, the order of magnitude for values are the same for the whole-model viscous dissipation plot and lithosphere viscous dissipation plot, having values with magnitude of 1e-9. Higher peaks found in the lithosphere viscous dissipation plot are related with the first and third model, and the same happens in the whole-model viscous dissipation plot. At 42.5 minutes the viscous dissipation in the whole-model reaches 8e-9 W/m, while the viscous dissipation in the lithosphere reaches almost 3e-9 W/m. Then, at 47.5 minutes, the second event in the whole-model had a viscous dissipation value that surpassed the 4e-9 W/m and in the lithosphere the value reached almost 2.5e-9 W/m. The third peak, that occurred before the 55 minutes, had a value of viscous dissipation in the whole-model of almost 9e-9 W/m, while the viscous dissipation in the lithosphere reached almost 3e-9 W/m. Finally, the last event had a value of almost 5e-9 W/m in the whole-model and ~ 1.5e-9 W/m of viscous dissipation in the lithosphere.

The subducted area plot (see **Figure 5-6e**) shows that before the dynamic starting the area subducted was already 5 cm^2 and in the first event of subduction at 42.5 minutes the area reached 15 cm^2. Then the plot kept constant until 47.5 minutes when the second event was formed and

reached more than 20 cm^2. The area remained constant until the next event at 55 minutes approximately and reached ~30 cm^2. Then, in the final event the subducted area reached more than 35 cm^2. At the end of the model, the full area was subducted. About the subduction rate plot (see **Figure 5-6f**), it shows the same behavior of peaks, the first event represents a high value, the second-one represents a lower value, then the third increases and the last-one scales down again. During the first event the maximum value of area subducted was almost 0.25 cm^2 and in the second event of subduction the maximum value of area subducted in an instant of time was less than 0.2 cm^2. Then, a bit more of 0.2 cm^2 was the maximum area subducted during the third event in an instant. And finally, the last event was less than 0.2cm^2.

Figure 5-6: Information plots about the time evolution of Model 3: a) Trench Advance, b) Plastic Strain, c) Viscous Dissipation of total model Asthenosphere-Lithosphere, d) Viscous Dissipation of Lithosphere only, e) Subducted area and f) Subduction Rate.

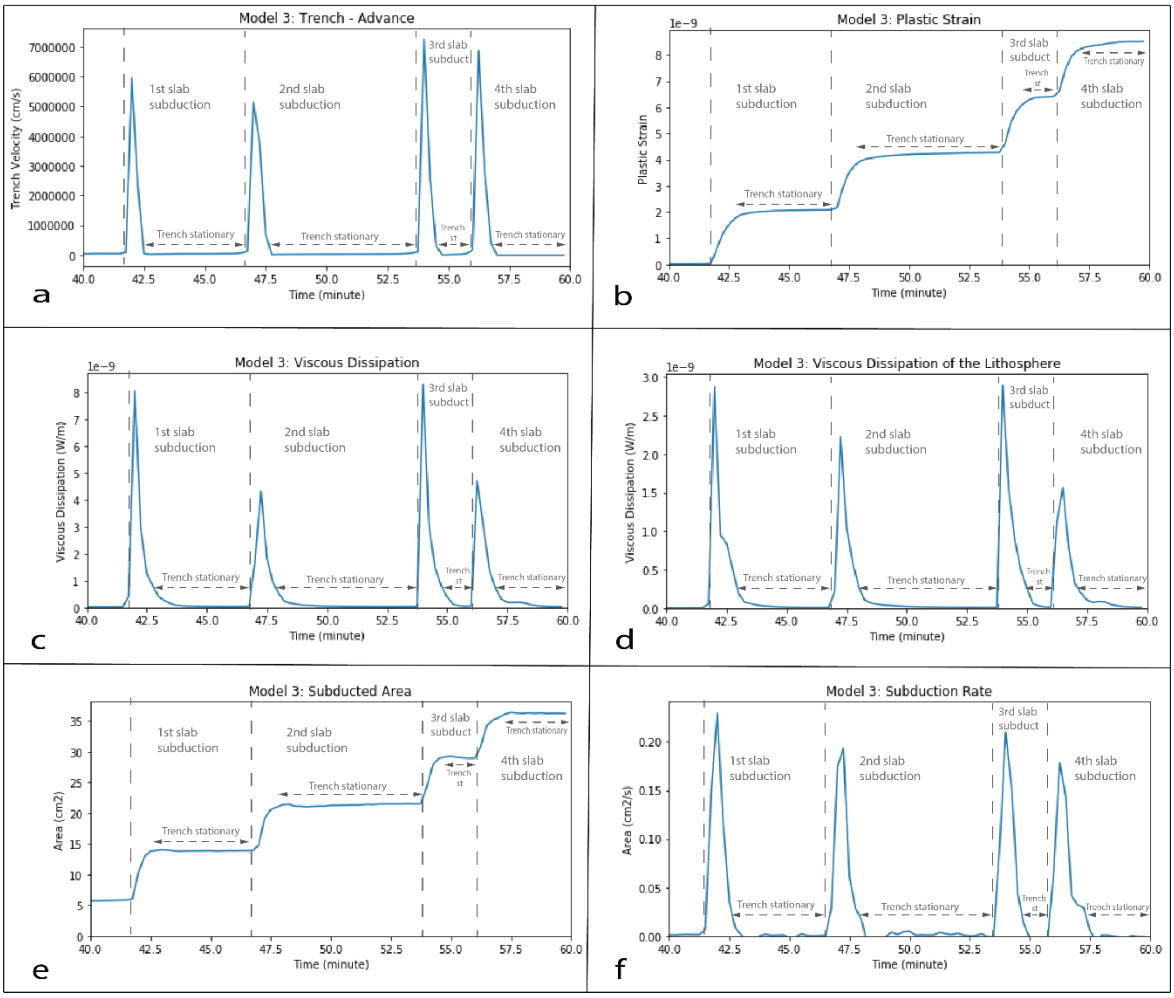

5.2. Analysis of results

In this section, I compare the impact of minor parameter changes on the final outcome of three models. The first parameter change evaluated was the bottom boundary condition and the second parameter is the lithosphere layer geometry.

In numerical models, it is usual to define a boundary condition at the bottom, linking it with the 660 km discontinuity. Quinquis et al. (2011) studied the influence of boundary conditions in numerical models of subduction that included the lower mantle to evaluate slabs behavior. That study stated that considering a free-slip boundary condition at the bottom makes easier the slab sliding and bending, and eventually, the slab folding; but considering a non-slip boundary condition, if lower mantle properties were defined and included in the dynamic system, the slab would be forced to try to penetrate the lower mantle.

Boundary conditions in numerical models are important because they are able to affect the subduction motion depending on the used far-field boundary condition (Capitanio et al., 2010). In this case, the variation of boundary conditions in the bottom of the model promoted some differences between Model 1 (frictionless behavior) and Model 2 (frictional behavior). Firstly, in Model 1 the slabs had the possibility to freely slide after hitting the bottom of the box, allowing the slab formed in the first event of subduction to spread before thinning out and breaking, in comparison with Model 2. For that reason, in Model 2 it is possible to observe that the first slab took less material from the lithosphere layer than the first slab in Model 1.

Also, the boundary condition of the bottom affected the time frame in which the models were developed. In Model 1 the initiation of motion was earlier than in Model 2, taking into consideration that dynamic in Model 1 started before 15.12 and finished after 15.15 hours, while Model 2 started after 15.12 and finished at almost 15.16 hours. That means that the boundary conditions at the bottom had influence in the dynamic of the system. Subsequently, it affected the values of velocities of trench advance, Model 1 being the one with higher speeds, smoother lithosphere subduction, and further advancement of the trench during the first slab. Basically, the influence of a frictionless boundary condition at the bottom resulted in a more dynamic system that

promoted farther slab sliding. In both Model 1 and Model 2, when events of subduction were finishing, the folded slabs increased their angle of subduction until being almost vertical and this caused a slight retreat in the trench during the last seconds of motion.

On the other hand, Model 3 had a large difference in the shape of the lithosphere layer. In this case, the lithosphere contained a gap of 2 cm that promoted the faster initiation of subduction in the system. For this model, the dynamic system promoted the weakness on the right edge of the lithosphere layer, because of the gap that allowed the push of the poloidal flows, thus the motion onset. The time needed for Model 3 to start subduction was considerably less than Model 1 and Model 2, because of the 2 cm gap nucleated deformation early on.

The formation of 4 different events of subduction in Model 3 consisted of slab thinning, promoting its breaking up after not having the possibility to continue sliding. The balanced dynamics of the system made the Model 3 to have lower values of velocity than the other two models. In general, all results from Model 3 were more uniform, in relation to the different events of subduction; for that reason, all peaks that represent each event have the same behavior in all plots. Also, values of viscous dissipation with the same order of magnitude, and the same peaks in the whole-model and lithosphere demonstrate that the system is better balanced.

All models have in common the slab tearings and this characteristic is also observed in the analogue model that was made for a Structural Geology class (see **Figure A-2**). In the analogue model, the slab tearings were related with short-lived events of subduction, however, in my numerical models the slab tearings are related with significant events of subduction.

Another similarity between the analogue and numerical models is the time scale. The analogue model took 6 min 36 s to start the subduction process and the dynamic had a duration of 1 min 26 s, this means that the time of onset of action was greater by about 4.6 times the time of duration of the subduction dynamics. Numerical Models 1 and 2 took around 15 hours to show significant changes and additionally the motion of the models had a duration of less than 11 minutes, this means that the time of onset of action has a time scale difference for around 81.8 times with the

time of duration of the subduction dynamics. Finally, Model 3 took 40 minutes to start the motion and took for about 15 minutes more to complete the subduction events, this means that the time of onset of motion was greater by about 2.6 times the time of duration of the subduction dynamics. By this way, it is possible to find relationships about the proportions of time scales between the analogue model and numerical Model 3, because the difference is less than double and much smaller than compared to Model 1 and Model 2.

About velocities, Capitanio et al., (2010) shows that it is possible to surpass velocities of 10 cm/yr in real subduction zones (S. Fiji and Izu-Bonin). In my numerical models, due to the high-density differences between the layers, they all show trench advance speeds of order of magnitude of ~ 1e6 and ~ 1e7 cm/s. So, the velocities in the small-scale numerical models are a congruent proportion of the maximum velocities registered in real conditions.

6. Conclusions

In conclusion, numerical models usually represent a limitation to undergraduate students because of the difficult access to the computational tools that it requires. However, in this work I show that numerical methods can be used at the under-graduate level and provide a practical guide that undergraduate students can easily use with their personal or student computers. Using this work as a point of reference, undergraduate students will be able to perform their own numerical models and get involved in the understanding of geodynamic processes such as subduction dynamics.

The models reported here demonstrate the influence of boundary conditions at the bottom. In Model 1, with a free-slip boundary condition at the bottom, the slab has the possibility to easily slip, spread further, and last longer; it also allows faster speeds of the trench advance. Model 2 in contrast, with a non-slip boundary condition at the bottom, causes slab folding as soon as the slab hits the bottom, which in turn promotes their earlier thinning and tearing, and trench advance lasts less. Regarding Model 3, an imposed gap in the lithosphere layer promoted the faster subduction onset, because it simulated a premeditated weakness in the system. So, this imposed gap represented a better-balanced numerical model, which had uniformity in trench advance speeds, congruence in viscous dissipation in the whole-model and lithosphere-only, and a periodic way of subducting the lithosphere. The trench advance velocities registered in the numerical models that relied on a high-density material that was dropped into a much less dense material, promoted a high order of magnitude of velocities (1e6 and 1e7), however these results can be a great small-scale representation of high subduction velocities in real conditions. Finally, all models demonstrated the functionality of numerical methods based on real properties extracted from a tangible situation, such as an analogue model with accessible materials. They also had similar behaviors in terms of multiple slab tearings. However, among all the models, the Model 3 is the one that has a better approached to the analogue model in terms of time scale.

A. Appendix: Results from Analogue Model

Figure A-1: Selected image captures of the evolution of the analogue model discussed in the text. Strain markers are numbered and tracked throughout the experiment. Elapsed time in each capture refers to the time elapsed since the initiation of motion.

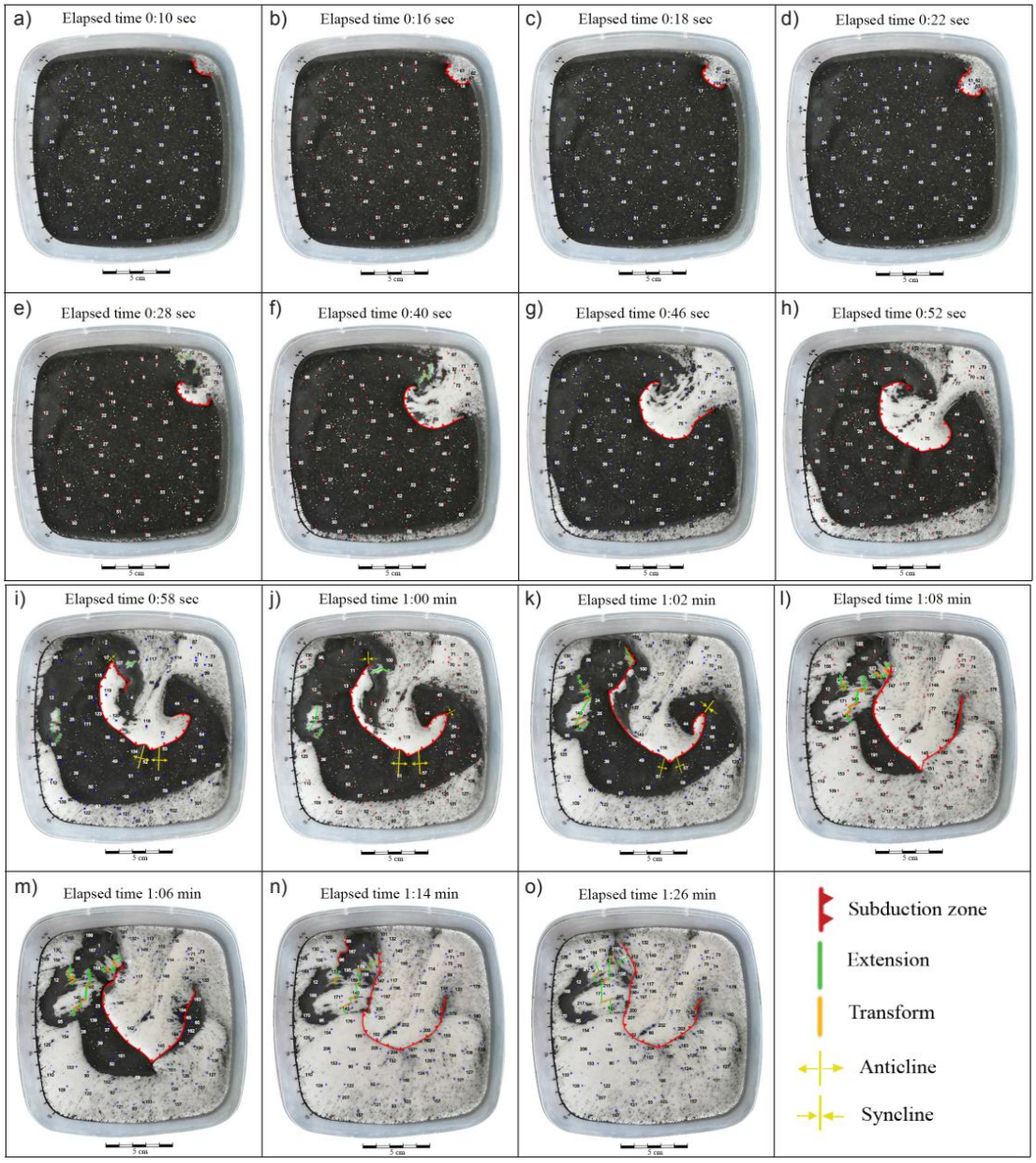

Figure A-2: Rate of subduction measured as area of the magnetic sand layer consumed every 2s. a) Cumulative plot of subducted area showing that trench advance and lengthening is characterized by a gradual increase in subduction rate. Once the trench becomes stationary, the subduction rate gradually slows down to zero. b) Instantaneous subduction rate measured as area lost in each image capture; note that the climax of subduction marks the moment that the trench becomes stationary when the black sand layer is being consumed in both sides of the subduction zone after vertical-axis rotation of 180° brings sand layer around the trench.

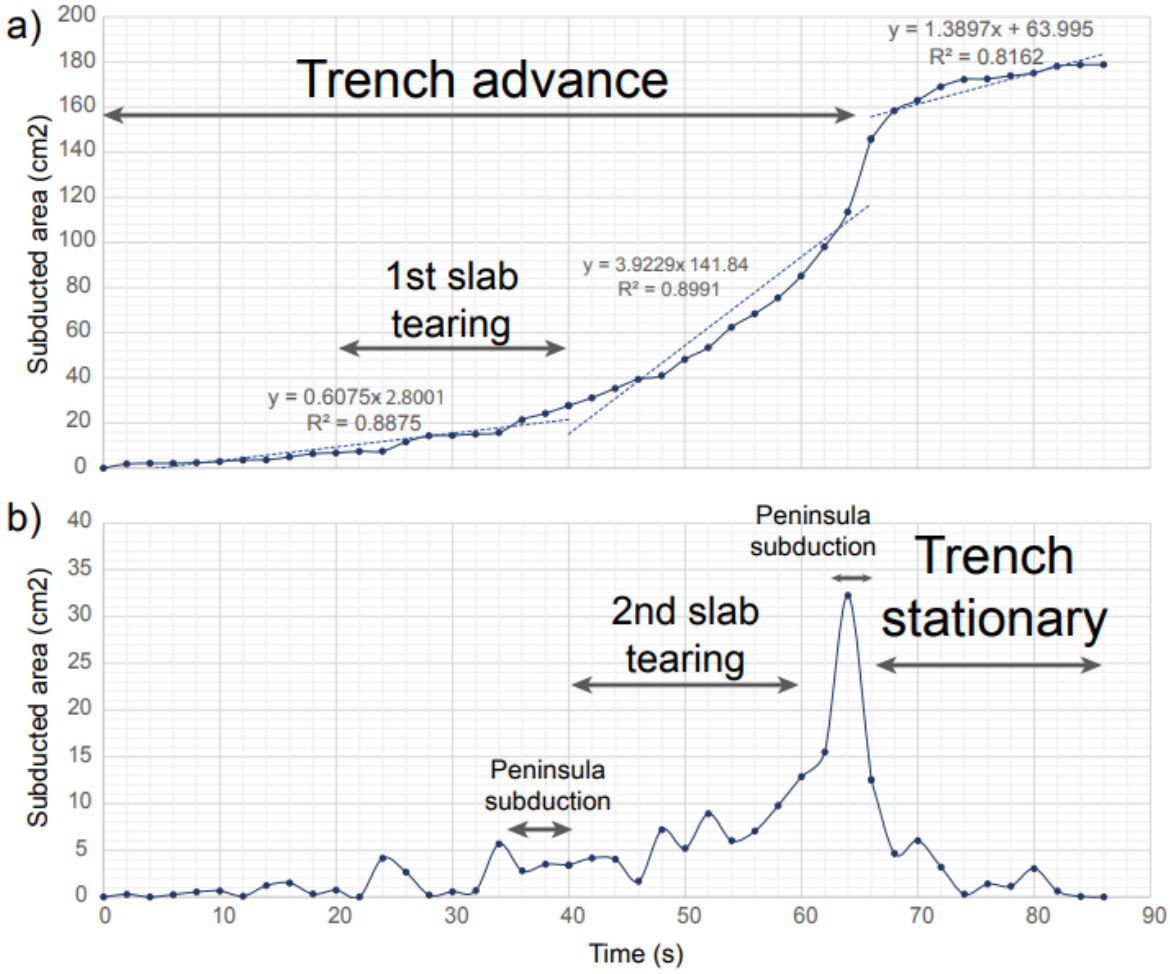

B. Appendix: Practical guide for structural geology class

This practical guide pretends to help undergraduate students to develop their own numerical models with real parameters or parameters of their preference. This, to promote the development of basic numerical models that simulates high-scales geodynamic processes, without major limitations.

1. Docker is an open platform for developing, shipping, and running applications. This is the software that you would use to create your own container and run your models. Download here: https://docs.docker.com/get-docker/. Be sure to confirm the system requirements.

2. After having the access to the software installed, go to your terminal, and paste *docker pull underworldcode/uwgeodynamics*

Wait until the image download is complete.

3. Go to Images > underworldcode/uwgeodynamics > run > optional settings:

Name your container

Local Host: 8887

Host Path: select the directory of your choice or create a new folder for your models

Container Path: /home/jovyan/workspace

4. Go to Containers. Select the new container and copy the token. Then, select open in the browser and paste the token. Now you have access to the Jupyter Notebook.

5. Go to 'Workspace', create a new Notebook Python 3 and add cells to paste the script that is shown below.

6. After running your models, you can visualize them in Paraview. Go to https://www.paraview.org/download/

7. In paraview, go to file > open > select the directory > XDMF.field…xmf > XDMF reader. To open tracers' files it is necessary to do the same process and select 'slab1.xmf'. *Slab1 is the

name of the file that saves information about one of the rows of tracers. You need to repeat the step for each row of tracers (slab 1, slab 2, slab 3). After adding files you need to press Apply to enable functions.

8. Active the view of files. Select projMaterialField to explore other parameters, such as density field, stress field, stress tensor, plastic strain, etc. Go to view > color map editor, to change color palettes, edit letter fonts, use log scale, etc.

9. Review Paraview User's Guide https://docs.paraview.org/en/latest/

```
#Import packages and functions needed
import UWGeodynamics as GEO
import numpy as np
from underworld import function as fn
from UWGeodynamics import visualisation as glucifer
from underworld import function as fn
u = GEO.UnitRegistry
import math
import numpy as np
import os
import scipy
```

```
#Here you define the units
GEO.rcParams["velocityField.SIunits"]= u.cm/u.sec
GEO.rcParams["timeField.SIunits"]= u.sec
GEO.rcParams["time.SIunits"]= u.sec
GEO.rcParams["projTimeField.SIunits"]= u.sec
```

```
#Materials values
mantleViscosity_asthenos=(21.7*u.pascals*u.second) #Here enter the viscosity of the viscous fluid material
slabViscosity_lithos=(10000*(21.7)*u.pascals*u.second) #Try to find the best proportion for the slab viscosity

mantleDensity_asthenos=1027* u.kilogram / u.meter**3
slabDensity_lithos=2286* u.kilogram / u.meter**3
```

```
#Scalling
#Units
u = GEO.UnitRegistry
#Rebecca et al., Scaling
dRho =   (slabDensity_lithos-mantleDensity_asthenos)
g    =   9.8 * u.meter / u.second**2
H    = 6.8 * u.centimeter
```

```
# lithostatic pressure for mass-time-length
ref_stress = dRho * g * H
# viscosity of upper mante for mass-time-length
ref_viscosity = mantleViscosity_asthenos
#References
ref_time        = ref_viscosity/ref_stress
ref_length      = H
ref_mass        = (ref_viscosity*ref_length*ref_time)

KL = ref_length
KM = ref_mass
Kt = ref_time

GEO.scaling_coefficients["[length]"] = KL
GEO.scaling_coefficients["[time]"] = Kt
GEO.scaling_coefficients["[mass]"]= KM
#Model Output Folder
outputPath= "Here you name the folder of your model"
dim=2

#Model Resolution
nEls=(70,45) #Here you can try better resolutions, however the model run will last longer

#Model Dimensions
boxLength = 28 * u.centimeter
boxHeight =  6.8 * u.centimeter

#Define your vertical unit vector using a python tuple
g_mag = 9.8 * u.meter / u.second**2

if dim == 2:
   minCoord   = (0., -boxHeight)
   maxCoord   = (boxLength, 0.)
   g_vec      = ( 0.0, -1.0 * g_mag )

else:
   minCoord   = (0., -boxHeight, 0.)
   maxCoord   = (boxLength, 0., boxWidth)
   g_vec      = ( 0.0, -1.0 * g_mag , 0.0 )

Model = GEO.Model(elementRes = nEls,
                  minCoord   = minCoord,
                  maxCoord   = maxCoord,
                  gravity    = g_vec,
                  outputDir  = outputPath)
```

```
#Here you have two options to run your models. The first one is the complete lithosphere layer and
the second one is a polygon with 4 vertices in the place of your choice
#Remember to comment the option you won´t use
```

```
#Option 1
#model Materials
mantle=Model.add_material(name="Mantle_asthenos", shape=GEO.shapes.Layer(top=Model.top,
bottom=Model.bottom))
slab=Model.add_material(name="slab_lithos", shape=GEO.shapes.Layer(top=0.*u.kilometer,
bottom=-1*u.centimeter)) #Here you can modify the lithosphere tickness

############################################################

#Option 2
#Here you define the vertices of the polygon
plate_shape=[(0 * u.cm, 0 * u.cm),
          (26 * u.cm,0 * u.cm),
          (26 * u.cm,-1 * u.cm),
         (0 * u.cm,-1 * u.cm),
]

plate_shape=GEO.shapes.Polygon(plate_shape)

#model Materials
mantle=Model.add_material(name="Mantle_asthenos", shape=GEO.shapes.Layer(top=Model.top,
bottom=Model.bottom))
slab=Model.add_material(name="slab_lithos", shape=plate_shape)
```

```
#Preview of 2D materials-Materials Field (from swarm)
Fig = glucifer.Figure(figsize=(1200,400))
Fig.Points(Model.swarm, Model.materialField,fn_size=2.0, discrete=True)
#Fig.Surface(Model.mesh,Model.projMaterialField,fn_size=2.0)
Fig.show()
```

```
#Viscosity
mantle.viscosity=mantleViscosity_asthenos
slab.viscosity=slabViscosity_lithos

slab.minViscosity=((21.7*10)*u.pascals*u.second) # Here you define the minimum viscosity that
could have the dynamic system

#Density
mantle.density=mantleDensity_asthenos
slab.density=slabDensity_lithos
```

```
#Plasticity
slab.plasticity=GEO.VonMises(cohesion=50.* u.pascals,cohesionAfterSoftening=30. * u.pascals)
#Here you define the plasticity of the lithosphere layer
#mantle.plasticity= #The mantle is only viscous
```

```
import os
try:
   os.mkdir(outputPath)
except FileExistsError:
   pass
```

```
#Time
#This part saves the time data of your models
store = glucifer.Store("store")
figure_one = glucifer.Figure(store, figsize=(1200,400))
figure_one.append(Fig.Points(Model.swarm, fn_colour=Model.materialField, opacity=0.5,
fn_size=2.0))
store.step = 0

fout = outputPath+'/FrequentOutput.dat'
if rank == 0:
   with open(fout,'a') as f:
       f.write('#step\t time(second)\t Vrms(cm/yr)\n')

def post_solve_hook():
   vrms = Model.stokes_SLE.velocity_rms()
   step = Model.step
   time = Model.time.m_as(u.second)



   if rank == 0:
      with open(fout,'a') as f:
         f.write(f"{step}\t{time:5e}\t{vrms:5e}\n")
      store.step += 1


Model.post_solve_functions["Measurements"] = post_solve_hook
```

```
#You work here on the passive tracers
def to2Darray(array_x,array_y):
   tracers=np.zeros((len(array_x),2))
   counter=0
   for i,j in zip(array_x,array_y):

      tracers[counter][0]=GEO.nd(i.magnitude* u.cm)
      tracers[counter][1]=GEO.nd(j.magnitude* u.cm)

      counter=counter+1
   return tracers

x=np.linspace(0,28,100)*u.cm #(y1, y2, number of tracers)
```

```
y=(x*0*u.cm)*u.cm
w=(x*0-0.5*u.cm)*u.cm          # depth of rows
z=(x*0-1*u.cm)*u.cm

slab1=Model.add_passive_tracers(name="Slab1",vertices=to2Darray(x,y))
slab2=Model.add_passive_tracers(name="Slab2",vertices=to2Darray(x,w))
slab3=Model.add_passive_tracers(name="Slab3",vertices=to2Darray(x,z))
```

```
Fig = glucifer.Figure(figsize=(1200,400))

Fig.Points(slab1, pointSize=5.0)
Fig.Points(slab2, pointSize=5.0)
Fig.Points(slab3, pointSize=5.0)
Fig.Points(Model.swarm, Model.materialField, fn_size=3.0)
Fig.show()
```

```
#Here you assign velocity fields to the tracers
slab1.add_tracked_field(Model.velocityField[0],
                        name="Subducting plate velocity_X",
                        units=u.centimeter/ u.year,
                        dataType="float")
slab1.add_tracked_field(Model.velocityField[1],
                        name="Subducting plate velocity_Y",
                        units=u.centimeter/ u.year,
                        dataType="float")

slab2.add_tracked_field(Model.velocityField[0],
                        name="Subducting plate velocity_X",
                        units=u.centimeter/ u.year,
                        dataType="float")
slab2.add_tracked_field(Model.velocityField[1],
                        name="Subducting plate velocity_Y",
                        units=u.centimeter/ u.year,
                        dataType="float")

slab3.add_tracked_field(Model.velocityField[0],
                        name="Subducting plate velocity_X",
                        units=u.centimeter/ u.year,
                        dataType="float")
slab3.add_tracked_field(Model.velocityField[1],
                        name="Subducting plate velocity_Y",
                        units=u.centimeter/ u.year,
                        dataType="float")
```

```
#Here you can modify the Velocity Boundary Conditions
#(x,y) None=free slip   0=non-slip
Model.set_velocityBCs(left=[0.,0.],  #left side of the box
```

```
                right=[0.,None],        # right side of the box
                bottom=[None, 0.],      #bottom of the box
                top=[None, 0.])         #top of the box
```

```
Model.init_model()
```

```
#Solver Parameters
Model.solver.set_inner_method("lu")
Model.solver.set_penalty(1e6)
GEO.rcParams["initial.nonlinear.tolerance"] = 1e-4
```

```
#Data to Save
outputss=['pressureField',
        'strainRateField',
        'velocityField',
         'projStressField',
          'projMaterialField',
        'projViscosityField',
        'projStressField',
          "projTimeField",
         'projPlasticStrain',
        'projDensityField',
        'projStressTensor',
        ]
GEO.rcParams['default.outputs']=outputss
```

```
#Duration of models
#Running Model (Time)
Model.run_for(duration=40.*u.minute,checkpoint_interval=10*u.minute)

#Running Model (Steps)
Model.run_for(nstep=400,checkpoint_interval=10)
```

```
#Preview of 2D materials-Materials Field (from swarm)
Fig = glucifer.Figure(figsize=(1200,400))
Fig.Points(Model.swarm, Model.materialField,fn_size=2.0, discrete=True)
#Fig.Surface(Model.mesh,Model.projMaterialField,fn_size=2.0)
Fig.show()
Fig.save("Figure.png")
```

Bibliography

Ahrens, James, Geveci, Berk, Law, Charles, ParaView: An End-User Tool for Large Data Visualization, Visualization Handbook, Elsevier, 2005, ISBN-13: 978-0123875822

Beucher, R., Moresi, L., Giordani, J., Mansour, J., Sandiford, D., Farrington, R., ... & Morón, S. (2019). UWGeodynamics: A teaching and research tool for numerical geodynamic modeling. Journal of Open Source Software, 4(36), 1136.

Capitanio, F., Morra, G., & Goes, S. (2007). Dynamic models of downgoing mantleplate-buoyancy driven subduction: Subduction motions and energy dissipation. Earth and Planetary Science Letters, 262(1-2), 284-297. https://doi.org/10.1016/j.epsl.2007.07.039

Capitanio, F. A., Stegman, D. R., Moresi, L. N., & Sharples, W. (2010). Upper plate controls on deep subduction, trench migrations and deformations at convergent margins. *Tectonophysics*, *483*(1–2), 80–92. https://doi.org/10.1016/j.tecto.2009.08.020

Capitanio, F. A., Gonzalez, C. M., & Brune, S. (2021). Numerical Modeling of Tectonic Processes. En Encyclopedia of Geology (pp. 903-912). Elsevier. https://doi.org/10.1016/B978-0-12-409548-9.12016-0

Cooper, C. M., Lenardic, A., & Moresi, L. (2004). The thermal structure of stable continental lithosphere within a dynamic mantle. Earth and Planetary Science Letters, 222(3-4), 807-817. https://doi.org/10.1016/j.epsl.2004.04.008

Delgado, J., López, J., Zárate, I., & Montes, C. (In review). Analogue Models of Subduction in the Kitchen

Faccenna, C., Becker, T. W., Holt, A. F., & Brun, J. P. (2021). Mountain building, mantle convection, and supercontinents: Revisited. Earth and Planetary Science Letters, 564, 116905. https://doi.org/10.1016/j.epsl.2021.116905

Funiciello, F., Faccenna, C., & Giardini, D. (2004). Role of lateral mantle flow in the evolution of subduction systems: Insights from laboratory experiments. Geophysical Journal International, 157(3), 1393–1406. https://doi.org/10.1111/j.1365-246X.2004.02313.x

Funiciello, F., Faccenna, C., Giardini, D., & Regenauer-Lieb, K. (2003). Dynamics of retreating slabs: 2. Insights from three-dimensional laboratory experiments: 3-D LABORATORY EXPERIMENTS OF SUBDUCTION. Journal of Geophysical Research: Solid Earth, 108(B4). https://doi.org/10.1029/2001JB000896

Gerya, T. (2011). Future directions in subduction modeling. *Journal of Geodynamics*, *52*(5), 344–378. https://doi.org/10.1016/j.jog.2011.06.005

Gerya, T. (2022). Numerical modeling of subduction: State of the art and future directions. *Geosphere*, *18*(2), 503–561. https://doi.org/10.1130/GES02416.1

Holtzman, B. K., Kohlstedt, D. L., & Morgan, J. P. (2005). Viscous Energy Dissipation and Strain Partitioning in Partially Molten Rocks. Journal of Petrology, 46(12), 2569-2592. https://doi.org/10.1093/petrology/egi065

Ismail-Zadeh, A., & Tackley, P. (2010). Computational Methods for Geodynamics. Cambridge University Press. 349.

Mansour, J., Giordani, J., Moresi, L., Beucher, R., Kaluza, O., Velic, M., ... & Beall, A. (2020). Underworld2: Python geodynamics modeling for desktop, hpc and cloud

Martinod, J., Funiciello, F., Faccenna, C., Labanieh, S., & Regard, V. (2005). Dynamical effects of subducting ridges: Insights from 3-D laboratory models. Geophysical Journal International, 163(3), 1137–1150. https://doi.org/10.1111/j.1365-246X.2005.02797

Moresi, L., Dufour, F. D. R., & Hlhaus, H.-B. M. (2002). Mantle Convection Modeling with Viscoelastic/Brittle Lithosphere: Numerical Methodology and Plate Tectonic Modeling. Pure Appl. Geophys., 159, 22.

Moresi, L., Dufour, F., & Mühlhaus, H.-B. (2003). A Lagrangian integration point finite element method for large deformation modeling of viscoelastic geomaterials. Journal of Computational Physics, 184(2), 476-497. https://doi.org/10.1016/S0021-9991(02)00031-1

Moresi, L., Quenette, S., Lemiale, V., Mériaux, C., Appelbe, B., & Mühlhaus, H.-B. (2007). Computational approaches to studying non-linear dynamics of the crust and mantle. Physics of the Earth and Planetary Interiors, 163(1-4), 69-82. https://doi.org/10.1016/j.pepi.2007.06.009

Moresi, L., Betts, P. G., Miller, M. S., & Cayley, R. A. (2014). Dynamics of continental accretion. Nature, 508(7495), 245-248. https://doi.org/10.1038/nature13033

Quinquis, M. E. T., Buiter, S. J. H., & Ellis, S. (2011). The role of boundary conditions in numerical models of subduction zone dynamics. *Tectonophysics*, *497*(1–4), 57–70. https://doi.org/10.1016/j.tecto.2010.11.001

Schellart, W. P., & Moresi, L. (2013). A new driving mechanism for backarc extension and backarc shortening through slab sinking induced toroidal and poloidal mantle flow: Results from dynamic subduction models with an overriding plate: MANTLE FLOW DRIVES BACKARC DEFORMATION. Journal of Geophysical Research: Solid Earth, 118(6), 3221-3248. https://doi.org/10.1002/jgrb.50173

Shearer, P. (1990). Seismic imaging of upper-mantle structure with new evidence for a 520-km discontinuity. Nature, 344(6262), 121-126. doi:10.1038/344121a0

Sobolev, S. V., Gruzinskaya, B., & Babeyko, A. Y. (2005). What drives orogeny in the Andes? 4.

Stead, D., Eberhardt, E., & Coggan, J. S. (2006). Developments in the characterization of complex rock slope deformation and failure using numerical modelling techniques. Engineering Geology, 83(1-3), 217-235. https://doi.org/10.1016/j.enggeo.2005.06.033

Stegman, D. R., Farrington, R., Capitanio, F. A., & Schellart, W. P. (2010). A regime diagram for subduction styles from 3-D numerical models of free subduction. Tectonophysics, 483(1–2), 29–45. https://doi.org/10.1016/j.tecto.2009.08.041

Walcott, R. I. (1970). Flexural rigidity, thickness, and viscosity of the lithosphere. Journal of Geophysical Research, 75(20), 3941-3954. https://doi.org/10.1029/JB075i020p03941

Yang, T., Moresi, L., Gurnis, M., Liu, S., Sandiford, D., Williams, S., & Capitanio, F. A. (2019). Contrasted East Asia and South America tectonics driven by deep mantle flow. Earth and Planetary Science Letters, 517, 106-116. https://doi.org/10.1016/j.epsl.2019.04.025

Zhang, Q., Guo, F., Zhao, L., & Wu, Y. (2017). Geodynamics of divergent double subduction: 3-D numerical modeling of a Cenozoic example in the Molucca Sea region, Indonesia: 3-D NUMERICAL MODELING OF DDS. Journal of Geophysical Research: Solid Earth, 122(5), 3977-3998. https://doi.org/10.1002/2017JB013991